An Assessment of Predictive Current Control Applied to the Direct Matrix Converter Based on SiC-MOSFET Bidirectional Switches

E. Maqueda, S. Toledo, R. Gregor, D. Caballero, F. Gavilán, J. Rodas
Faculty of Engineering
Universidad Nacional de Asunción
Luque, Paraguay
emaqueda@ing.una.py

M. Rivera
Faculty of Engineering
Universidad de Talca
Curicó Chile
marcoriv@utalca.cl

P. Wheeler
Dep. of Electrical and Electronic Engineering
University of Nottingham
Nottingham, UK
pat.wheeler@nottingham.ac.uk

***Abstract*—Matrix converters are devices that allow the management of bidirectional flows of energy with reduced size, increased useful life and high efficiency in ac-ac energy conversion systems. In this paper the experimental results obtained after the application of a predictive current control technique for a SiC-MOSFET based direct matrix converter feeding an isolated load are presented. The results obtained are compared with a scheme based on IGBT technology in terms of power consumption and total harmonic distortion.**

***Index Terms*—Matrix converter, predictive current control, SiC-MOSFET technology**

I. Introduction

Nowadays, the direct matrix converter (MC) is one of the most studied devices in AC-AC power conversion systems. The topologies of the MC offer a direct acac conversion and due to the absence of dc-link capacitors they are more compact and robust. They simultaneously achieve sinusoidal input and output waveforms as well as bidirectional power flow [1], [2]. Compared to a conventional back-to-back inverter (BTB), which requires bulky storage elements, the space saved by a MC has been estimated as a factor of three. The main applications are portable generation systems, for instance in variable speed diesel generation, variable speed wind-diesel topologies, distributed generation applications, emergency vehicles, military and aerospace applications, external elevators for building construction, and skin-pass mills flow [1], [3], [4]. MC are devices constructed from bidirectional switches (Bi-Sw) that have several advantages over their (BTB) counterparty, such as smaller size, less weight and management of bidirectional flows [5]. As for the technology used in manufacturing the Bi-Sw, there are mainly two types of semiconductors, IGBTs and those based on silicon carbide technology SiC-MOSFET [6], [7]. Generally, the preferred technology has been based on IGBT and discrete diodes. However, nowadays the trend points out towards the use of SiC-MOSFETs devices, since in comparison to IGBTs, they report lower losses in switching and conduction, and can even operate at higher frequency and voltage levels [8]. In general, the integration of semiconductors is sought in a single power module, due to the fact that through this integration it is possible to optimize spaces as well as handle higher power density. As for the operation of the MC it is preferable that the switching occurs at a high frequency in order to decrease the size of the passive components of the filters, SiC-MOSFETs are ideal for this application. In [9]–[11] a comparative analysis is made between the SiC-MOSFET and the IGBT applied in the MC, but operating in a control scheme based on modulation techniques, that do not possess the variable switching frequency characteristic of predictive control. In recent years, predictive current control applied to matrix converters has caught the attention of researchers [12], [13]. This article presents the results of the setup and experimental implementation of a predictive current control scheme for a three-phase MC based on SiC-MOSFET technology feeding an isolated load and the comparison of the perform of the system and another one based on IGBT technology. The control is implemented using the dSPACE 1103 to solve the algorithm and to determine the optimum vector to be applied at the next sampling time. While the optimal vector application and the switching strategy are carried out in a FPGA Nexys 3. The main contribution of this paper lies in the experimental comparison between IGBT technologies and SiC-MOSFET based technologies in terms of power consumption in the same conditions of input voltages and output currents under a predictive control scheme and the study of variation of the total harmonic distortion (THD) with increasing sampling frequency for both cases.

II. Proposed control topology

The proposed control scheme is presented by means of Fig. 1 which consists of a three-phase AC-AC conversion scheme using a MC in the power stage as the feeder of an isolated load. The implemented control technique is the model based predictive control (MPC) which will be described below.

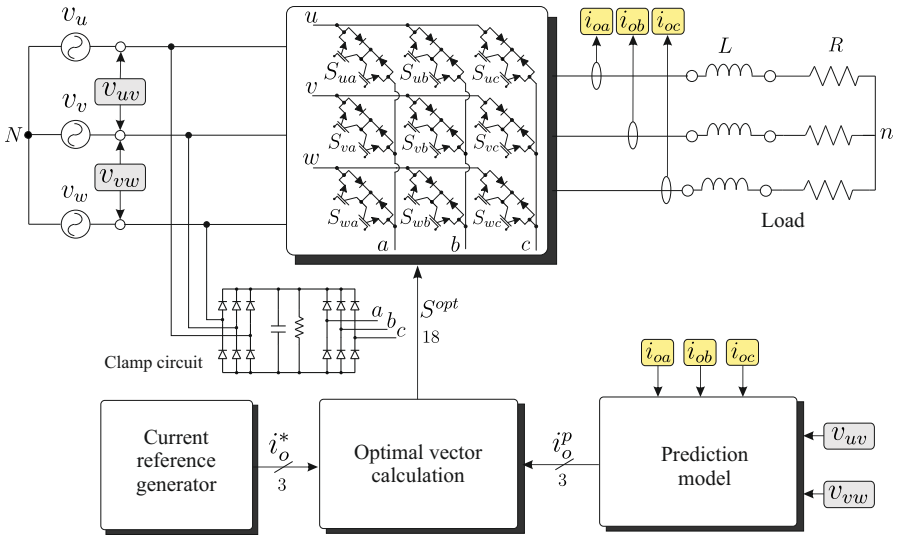

Fig. 1. Proposed experimental setup

A. Direct Matrix Converter. Basic principles

The switching function for a single switch is defined as [14]:

$$S_{ij} = \begin{cases} 0, & \text{if switch } S_{ij} \text{ is off} \\ 1, & \text{if switch } S_{ij} \text{ is on} \end{cases} \tag{1}$$

where $i \in \{u, v, w\}$ indicates the corresponding entry, $k \in \{a, b, c\}$ refers to the corresponding output. Considering that the inputs should never be short-circuited and that currents should never be interrupted abruptly, the restrictions are expressed as follows:

$$S_{ui} + S_{vi} + S_{wi} = 1, \quad \forall i \in \{a, b, c\}. \tag{2}$$

Under these constraints, the three-phased MC has 27 allowed switching states, out of the possible 512 (2^9). If the load and source are referenced with respect to the neutral point (N), then it is possible to describe the relation between the inputs and outputs of the voltage and current as follow:

$$\begin{bmatrix} v_a(t) \\ v_b(t) \\ v_c(t) \end{bmatrix} = \begin{bmatrix} S_{ua}(t) & S_{va}(t) & S_{wa}(t) \\ S_{ub}(t) & S_{vb}(t) & S_{wb}(t) \\ S_{uc}(t) & S_{vc}(t) & S_{wc}(t) \end{bmatrix} \begin{bmatrix} v_u(t) \\ v_v(t) \\ v_w(t) \end{bmatrix}, \tag{3}$$

$$\begin{bmatrix} i_u(t) \\ i_v(t) \\ i_w(t) \end{bmatrix} = \begin{bmatrix} S_{ua}(t) & S_{ub}(t) & S_{uc}(t) \\ S_{va}(t) & S_{vb}(t) & S_{vc}(t) \\ S_{wa}(t) & S_{wb}(t) & S_{wc}(t) \end{bmatrix} \begin{bmatrix} i_{oa}(t) \\ i_{ob}(t) \\ i_{oc}(t) \end{bmatrix}. \tag{4}$$

B. Predicitive Control in the Direct Matrix Converter

MPC has been applied in chemical and industrial processes for several years, mainly because these are complex but highly slow-moving processes [15], [16]. Electronic power devices also have complex models but with faster dynamics. However, the capacity and speed of microcontrollers have improved greatly, making feasible the modeling of discrete systems and the processing of electrical signals. All of the above contributes to the development of MPC control strategy in power electronics applications. On the other hand, one of the most attractive characteristics of the MPC is its intuitive and logical procedure of exposing the control problem, which makes it easy to understand and easy concept to implement.

One of the main elements to implement a MPC control strategy is a precise model of the system in order to have an adequate prediction. The model depends directly on the application of the controller [17]. In the case of power converters, these are composed of semiconductors that operate in only two states: cut and saturation. Therefore, there is always a finite number of possible combinations of the switching states in any power converter. This feature greatly simplifies the application of the MPC since because instead of having to waste time on a continuous optimization algorithm, it is possible to perform the direct evaluation of all possible switching states and select the best combination to use, according to the proposed control objectives.

The control objectives in power electronics are, generally, the tracking of currents, voltages, power, torque, flux, etc. [18]. These objectives are represented in the MPC through a cost function, which evaluates the errors between the references and the actual values of the variables of interest. Furthermore, it is possible to add some additional control objectives such as temperature control and minimization of switched and conduction losses [19], common mode voltages reduction [20], among others. Nowadays, it is possible to find in the market a vast variety of highly powerful microprocessors, which make a large number of calculations. These calculations are so fast that they can predict the behavior of variables such as real time current and voltage without a noticeable effect on the system under control, allowing the application of MPC in power electronics. The operational principle of this strategy is based on the prediction of the behavior of a system using its mathematical model and the optimization of a defined cost

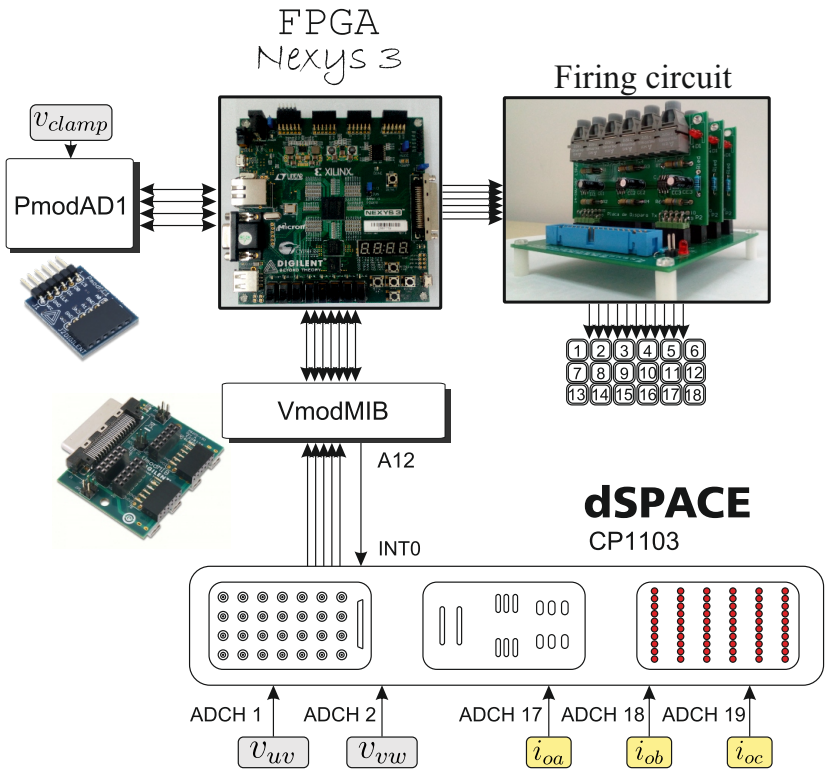

Fig. 2. Three-phase matrix converter controller setup.

function using the predicted values as a way to meet the control objectives. Applied to power converters it is possible to separate this operating principle in three steps: (i) calculation of the predicted variables using a discrete model, (ii) the evaluation of the cost function for each of the valid states of the converter, and (iii) the selection and application of the optimal switching state. These steps are present in all MPC schemes, since it is possible to modify each one independently to adjust the control scheme to any configuration.

C. Predictive Load Current Control in a Three-phase Matrix Converter

The conversion system is shown in Fig. 1. In order to control the current in the load (i_o), a mathematical model must be obtained that describes the dynamics in the load. The dynamics of the current in the load is defined by the following equation:

$$\frac{d\mathbf{i}_o(t)}{dt} = -\frac{R}{L}\mathbf{i}_o(t) + \frac{1}{L}\left(\mathbf{v}_o(t) - \mathbf{v}_{nN}(t)\right), \tag{5}$$

where:

$$\mathbf{i}_o(t) = \begin{bmatrix} i_{oa}(t) \\ i_{ob}(t) \\ i_{oc}(t) \end{bmatrix}, \quad \mathbf{v}_o(t) = \begin{bmatrix} v_{aN}(t) \\ v_{bN}(t) \\ v_{cN}(t) \end{bmatrix} \quad \mathbf{v}_{nN}(t) = \begin{bmatrix} v_{nN}(t) \\ v_{nN}(t) \\ v_{nN}(t) \end{bmatrix}, \tag{6}$$

And v_{nN} is determined based on the following equation:

$$v_{nN} = \frac{1}{3}\left(v_{aN} + v_{bN} + v_{cN}\right). \tag{7}$$

The discrete model is obtained by applying the Euler method in the equation (5), as follows:

$$\mathbf{i}_o(k+1) = \left(1 - \frac{RT_s}{L}\right)\mathbf{i}_o(k) + \frac{T_s}{L}\left(\mathbf{v}_o(k) - \mathbf{v}_{nN}(k)\right), \tag{8}$$

where T_s is the sampling time, R is the load resistance and L is the load inductance. The values of $\mathbf{v}_o(k)$ are obtained from the equation (3) for each of the 27 feasible switching combinations in order to evaluate the cost function and to select the combination that minimizes it. In general, the Clarke transform is used [21], which converts the three-phase balanced system (three components to calculate) to one simpler two-component α—β frame, through the following way:

$$\begin{aligned} x_\alpha &= \frac{2}{3}\left(x_a - 0.5x_b - 0.5x_c\right), \\ x_\beta &= \frac{2}{3}\left(\frac{\sqrt{3}}{2}x_b - \frac{\sqrt{3}}{2}x_c\right), \end{aligned} \tag{9}$$

being x_a, x_b y x_c the three-phase components and x_α and x_β the components of the new coordinates α—β. To define the cost function that achieves current tracking, the components α—β of the reference current $\mathbf{i}_o^*$ must be determined and compared with the predicted currents $\mathbf{i}_o^p$.

However, due to the optimal vector calculated in the k instant is applied in $k+1$, the controller has a delay of one sampling time and it is necessary to control the behavior in $k+2$ to avoid the effect of this issue. That is, using the predictive model (8) in k with the measurements in this instant

and the MC output voltage for the optimal vector calculated in $k-1$, then:

$$\mathbf{i}^{p}_{o\alpha\beta} = \left(1 - \frac{RT_s}{L}\right)\mathbf{i}_{o\alpha\beta} + \frac{T_s}{L}\left(\mathbf{v}_{opt\alpha\beta} - \mathbf{v}_{nN\alpha\beta}\right), \quad (10)$$

Then, the predicted current in $k+2$ is calculated base on $\mathbf{i}^{p}_{o}$ for every valid switching state vector using the follow equation:

$$\mathbf{i}^{p}_{o\alpha\beta2}(j) = \left(1 - \frac{RT_s}{L}\right)\mathbf{i}^{p}_{o\alpha\beta} + \frac{T_s}{L}\left(\mathbf{v}_{o\alpha\beta}(\mathbf{S}(j)) - \mathbf{v}_{nN\alpha\beta}\right), \quad (11)$$

where j represent everyone of the 27 switching combinations. Finally, the proposed cost function to achieve current control is:

$$g = (i^{*}_{\alpha} - i^{p}_{o\alpha2})^2 + (i^{*}_{\beta} - i^{p}_{o\beta2})^2, \quad (12)$$

Where i^{*}_{α} and i^{*}_{β} correspond to the components α—β of the reference current. The vector $S(j)$ which minimize g corresponds to the optimal vector that will be applied in the next sampling time.

It is convenient to mention also that, for the implementation of the MPC, the measurements of the line voltages of source v_{uv} and v_{vw} are taken, from which is possible to calculate the phase voltages v_u, v_v and v_w applying the following equations:

$$v_u = \frac{2}{3}\left(v_{uv} + \frac{1}{2}v_{vw}\right), \quad (13)$$

$$v_v = \frac{2}{3}\left(v_{vw} + \frac{1}{2}v_{wu}\right), \quad (14)$$

$$v_w = -v_u - v_v. \quad (15)$$

III. Description of the Bidirectional Switch Design and Experimental Platform

This section describes the design and implementation of the bidirectional switch used to construct the MC and presents the main experimental results obtained.

A. Bidirectional switch design

The design of the bidirectional switch has been based on the electrical diagram shown in Fig. 3. The Fig. 3(a) shows of the diagram corresponds to the bidirectional switch control circuit consisting mainly of the gate semiconductor gate controller and the optical fiber receiver modules, which receive the PWM control signal and send it to the input of the ICs gate controller, the output of the control circuit is connected to the power circuit which is observed on the Fig. 3(b) of the diagram, formed mainly by SiC-MOSFET power semiconductors, for this design, and polarization resistors. The control board is independent of the power board. The modular scheme makes the circuit to be simple to replace en case of failures.

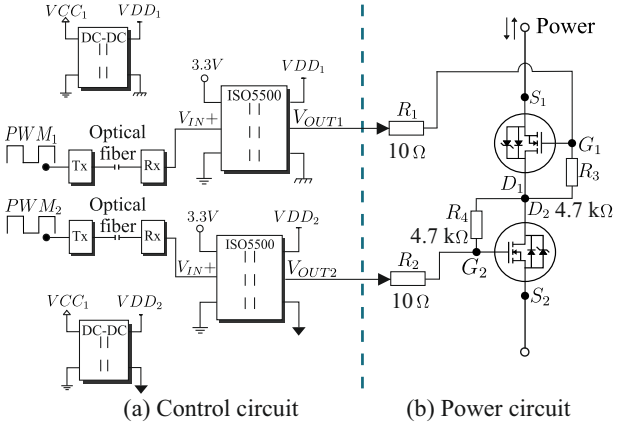

Fig. 3. Electric diagram of the bidirectional switch. (a) Control circuit and (b) Power circuit

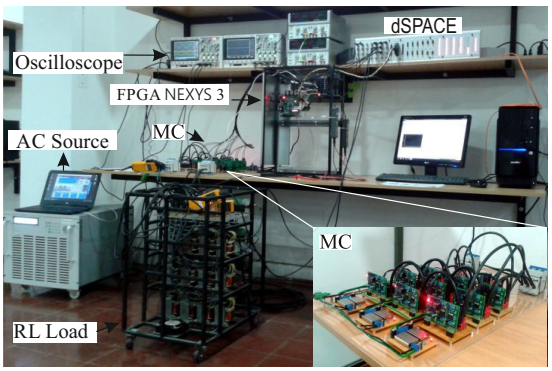

Fig. 4. Experimental setup using SiC MOSFET technology in the MC

B. Description of the experimental platform and obtained results

The experimental platform consists of a scheme that feeds a three-phase load from a source by means of an MC as shown in Fig. 2. The control scheme was implemented using the dSPACE CP1103 as the control device for optimal vector computing, communicated with a Nexys 3 FPGA in which the appropriate switching strategy is executed and the control signals are sent to the 18 switches according to the calculated vector and using optical transmission. Fig. 4 shows the experimental platform.

Posterior to assembling the two schemes with the parameters shown in Tabla I, both showed a correct operation, however the best result was obtained with the SiC-MOSFET-based scheme and is shown in Fig 5. The maximum achieved reference current was of 8 [A] peak with a maximum power around 1,2 [kW]. As for the transient response, Fig. 6 denotes the step response for the MC with IGBTs and Fig. 7 shows the response of the system to a variation in the referenced current amplitude for the MC with SiC-MOSFETs. In both cases it is possible to observe the correct tracking and satisfyingly fast response times. The input power required by each of the schemes at different sampling frequencies is shown in Fig. 8

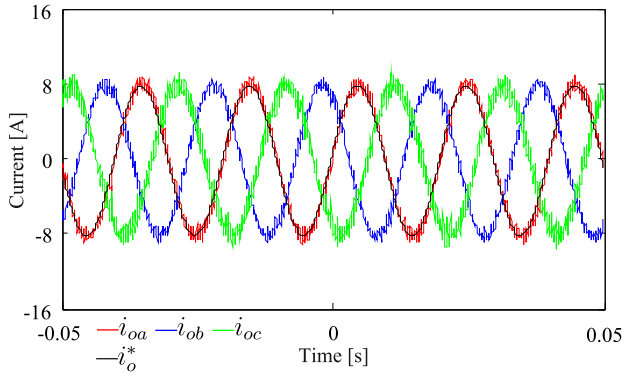

Fig. 5. Output current obtained in the SiC MOSFET MC for 1,2 kW.

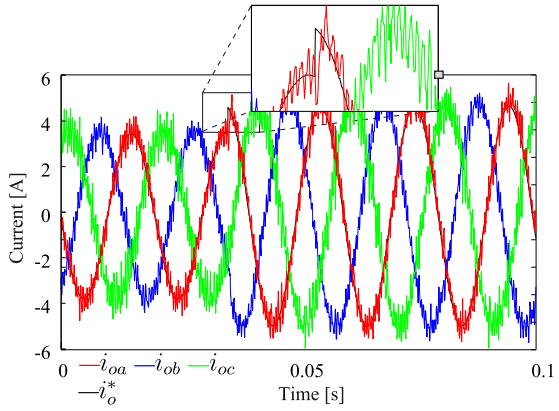

Fig. 6. Dynamic output current response of the IGBT MC for a step with $T_s = 100\ \mu s$.

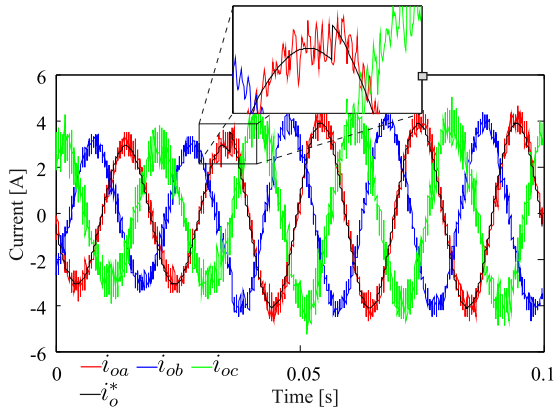

Fig. 7. Dynamic output current response of the SiC MOSFET MC for a step with $T_s = 100\mu s$.

TABLE I
PARAMETERS OF THE EXPERIMENTAL SETUP AND THE CONTROLLER.

	Experimental Parameters		
Description	Symbol	Value	Unit
Load resistence	R	10	Ω
Load inductance	L	13	mH
Source voltage	V_s	0-125	V_{rms}
Source frequency	f_s	50	Hz

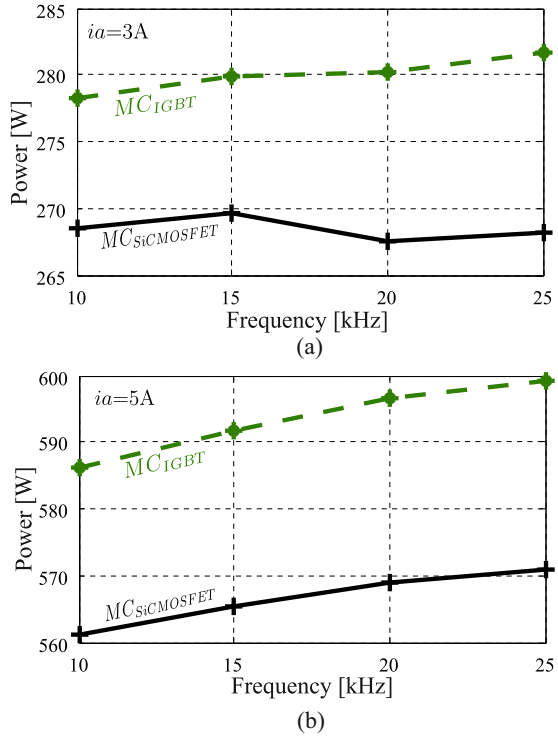

Fig. 8. Comparison between required power for distinct sampling frequencies and output currents.

when the same output current is requested. It is possible to observe that the SiC-MOSFET technology requires lower input power for the different frequencies when the same current is requested in the load.

Finally, the THD for both schemes at different sampling frequencies is shown in Fig. 9, it is possible to appreciate that there are no significant differences in this particular item.

IV. CONCLUSIONS

After completion of the work, it was possible to verify, in the first term, the correct functioning of the current predictive control scheme, both for the system with IGBT switches and for the one employing SiC-MOSFET technology. A power near 1,2 kW was achieved with currents of 1 to 8 [A] using SiC-MOSFETs, and between 1 to 5 [A] with IGBT switches. In addition, it was observed that for the same values of the required output current the SiC-MOSFETs had consumed less power, which leads to the conclusion that this proposal means a lower energy consumption at the input in order to reach the

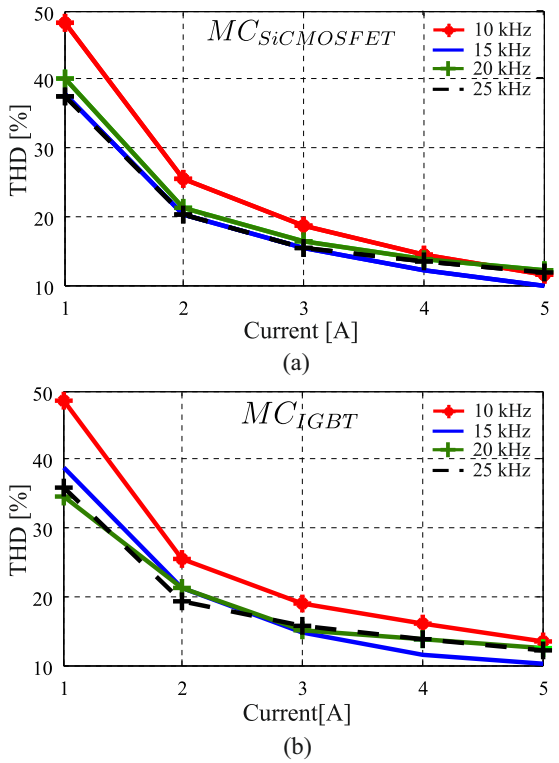

Fig. 9. THD values for different currents and sampling frequencies.

same desired values at the output. As for THD, there were no significant differences between the designs. The lack of a filter is the cause of the high THD value, which is expected to improve in a subsequent implementation. The SiC-MOSFET technology is most efficient in terms of power consumption in this experiment and it was possible to reach a current of 8 [A], which is highly superior than that achieved with the IGBT scheme.

AKNOWLEDGMENTS

The authors are grateful for the financial support of the Newton Picarte Project EPSRC: EP/N004043/1: New Configurations of Power Converters for Grid Interconnection Systems/CONICYT DPI20140007, Project FONDECYT Regular 1160690 and CONACYT of Paraguay through Project 14-INV-097 CONACYT-FIUNA.

REFERENCES

[1] C. F. Garcia, M. E. Rivera, J. R. Rodriguez, P. W. Wheeler, and R. S. Pena, "Predictive current control with instantaneous reactive power minimization for a four-leg indirect matrix converter," *IEEE Transactions on Industrial Electronics*, vol. 64, no. 2, pp. 922–929, 2017.

[2] M. Siami, D. A. Khaburi, M. Rivera, and J. Rodriguez, "An experimental evaluation of predictive current control and predictive torque control for a pmsm fed by a matrix converter," *IEEE Transactions on Industrial Electronics*, 2017.

[3] Y. Sun, W. Xiong, M. Su, X. Li, H. Dan, and J. Yang, "Topology and modulation for a new multilevel diode-clamped matrix converter," *IEEE Transactions on Power Electronics*, vol. 29, no. 12, pp. 6352–6360, 2014.

[4] S. M. M. Sangdehi, S. Hamidifar, and N. C. Kar, "A novel bidirectional dc/ac stacked matrix converter design for electrified vehicle applications," *IEEE Transactions on Vehicular Technology*, vol. 63, no. 7, pp. 3038–3050, 2014.

[5] P. Wheeler, J. Rodriguez, J. C. Clare, L. Empringham, and A. Weinstein, "Matrix converters: a technology review," *IEEE Transactions on Industrial Electronics*, vol. 49, no. 2, pp. 276–288, Apr 2002.

[6] A. Trentin, L. Empringham, L. de Lillo, P. Zanchetta, P. Wheeler, and J. Clare, "Experimental efficiency comparison between a direct matrix converter and an indirect matrix converter using both si igbts and sic mosfets," *IEEE Transactions on Industry Applications*, vol. 52, no. 5, pp. 4135–4145, Sept 2016.

[7] K. Koiwa and J. I. Itoh, "A maximum power density design method for nine switches matrix converter using sic-mosfet," *IEEE Transactions on Power Electronics*, vol. 31, no. 2, pp. 1189–1202, Feb 2016.

[8] S. Hazra, A. De, L. Cheng, J. Palmour, M. Schupbach, B. A. Hull, S. Allen, and S. Bhattacharya, "High Switching Performance of 1700-V, 50-A SiC Power MOSFET Over Si IGBT/BiMOSFET for Advanced Power Conversion Applications," *IEEE Trans. Power Electron.*, vol. 31, no. 7, pp. 4742–4754, Jul 2016.

[9] S. Safari, A. Castellazzi, and P. Wheeler, "Experimental and Analytical Performance Evaluation of SiC Power Devices in the Matrix Converter," *IEEE Trans. Power Electron.*, vol. 29, no. 5, pp. 2584–2596, may 2014.

[10] A. Trentin, L. De Lillo, L. Empringham, P. Wheeler, and J. Clare, "Experimental comparison of a direct matrix converter using Si IGBT and SiC MOSFETs," *IEEE Journal of Emerging and Selected Topics in Power Electronics*, vol. 3, no. 2, pp. 542–554, Jun 2015.

[11] A. Trentin, L. Empringham, L. De Lillo, P. Zanchetta, P. Wheeler, and J. Clare, "Experimental efficiency comparison between a direct matrix converter and an indirect matrix converter using both Si IGBTs and SiC MOSFETs," *IEEE J. Electron Devices Soc.*, vol. 52, no. 5, pp. 4135–4145, Sept 2016.

[12] S. Toledo, M. Rivera, R. Gregor, J. Rodas, and L. Comparatore, "Predictive current control with reactive power minimization in six-phase wind energy generator using multi-modular direct matrix converter," in *2016 IEEE ANDESCON*, Oct 2016, pp. 1–4.

[13] M. Rivera, P. Wheeler, A. Olloqui, and D. A. Khaburi, "A review of predictive control techniques for matrix converter - Part II," in *2016 7th Power Electronics and Drive Systems Technologies Conference (PEDSTC)*, Feb 2016, pp. 589–595.

[14] M. Venturini and A. Alesina, "The generalised transformer: A new bidirectional, sinusoidal waveform frequency converter with continuously adjustable input power factor," in *1980 IEEE Power Electronics Specialists Conference*, Jun 1980, pp. 242–252.

[15] W. Wang, W. Long, and L. Hu, "Nonlinear model predictive control of ph in rolling mill wastewater treatment," in *2009 International Workshop on Intelligent Systems and Applications*, May 2009, pp. 1–5.

[16] H. Han and J. Qiao, "Nonlinear model-predictive control for industrial processes: An application to wastewater treatment process," *IEEE Transactions on Industrial Electronics*, vol. 61, no. 4, pp. 1970–1982, Apr 2014.

[17] S. Kouro, M. A. Perez, J. Rodriguez, A. M. Llor, and H. A. Young, "Model predictive control: Mpc's role in the evolution of power electronics," *IEEE Industrial Electronics Magazine*, vol. 9, no. 4, pp. 8–21, Dec 2015.

[18] S. Vazquez, J. I. Leon, L. G. Franquelo, J. Rodriguez, H. A. Young, A. Marquez, and P. Zanchetta, "Model predictive control: A review of its applications in power electronics," *IEEE Industrial Electronics Magazine*, vol. 8, no. 1, pp. 16–31, Mar 2014.

[19] J. Falck, M. Andresen, and M. Liserre, "Thermal-based finite control set model predictive control for igbt power electronic converters," in *2016 IEEE Energy Conversion Congress and Exposition (ECCE)*, Sept 2016, pp. 1–7.

[20] H. Gao, B. Wu, D. . Xu, M. Pande, and R. P. Aguilera, "Common-mode-voltage-reduced model-predictive control scheme for current-source-converter-fed induction motor drives," *IEEE Transactions on Power Electronics*, vol. 32, no. 6, pp. 4891–4904, Jun 2017.

[21] L. Zhan, Y. Liu, and Y. Liu, "A Clarke transformation-based DFT phasor and frequency algorithm for wide frequency range," *IEEE Transactions on Smart Grid*, vol. PP, no. 99, pp. 1–1, 2017.